Protein Expression and Purification 176 (2020) 105742

Contents lists available at ScienceDirect

Protein Expression and Purification

journal homepage: www.elsevier.com/locate/yprep

# Expression, purification and crystallization of CLK1 kinase – A potential target for antiviral therapy

Noa Dekel [a], Yael Eisenberg-Domovich [a], Alexander Karlas [c], Thomas F. Meyer [d], Franz Bracher [e], Mario Lebendiker [a], Tsafi Danieli [a], Oded Livnah [a,b,*]

[a] The Wolfson Centre for Applied Structural Biology, The Hebrew University of Jerusalem, Jerusalem 91904, Israel
[b] Department of Biological Chemistry, Alexander Silverman Institute of Life Sciences, The Edmond J. Safra Campus, The Hebrew University of Jerusalem, Israel
[c] Viral Vaccines Development, ProBioGen AG, Berlin, Germany
[d] Max Planck Institute for Infection Biology, Department of Molecular Biology, Charitéplatz 1, 10117, Berlin, Germany
[e] Ludwig-Maximilians University, Department of Pharmacy-Center for Drug Research, Butenandstrasse 5-13, 81377, Munich, Germany

ARTICLE INFO

*Keywords:*
Influenza
Chikungunya
Viral infection
CLK1
Crystallization
Bacterial expression
Purification
Protein kinase
De-phosphorylation

ABSTRACT

Cdc-like kinase 1 (CLK1) is a dual-specificity kinase capable of autophosphorylation on tyrosine residues and Ser/Thr phosphorylation of its substrates. CLK1 belongs to the CLK kinase family that regulates alternative splicing through phosphorylation of serine-arginine rich (SR) proteins. Recent studies have demonstrated that CLK1 has an important role in the replication of influenza A and chikungunya viruses. Furthermore, CLK1 was found to be relevant for the replication of HIV-1 and the West Nile virus, making CLK1 an interesting cellular candidate for the development of a host-directed antiviral therapy that might be efficient for treatment of newly emerging viruses. We describe here our attempts and detailed procedures to obtain the recombinant kinase domain of CLK1 in suitable amounts for crystallization in complex with specific inhibitors. The key solution for the reproducibility of crystals resides in devising and refining expression and purification protocols leading to homogeneous protein. Co-expression of CLK1 with λ-phosphatase and careful purification has yielded crystals of CLK1 complexed with the KH-CB19 inhibitor that diffracted to 1.65 Å. These results paved the path to the screening of more structures of CLK1 complexed compounds, leading to further optimization of their inhibitory activity. Moreover, since kinases are desired targets in numerous pathologies, the approach we report here, the co-expression of kinases with λ-phosphatase, previously used in other kinases, can be adopted as a general protocol in numerous kinase targets for obtaining reproducible and homogenic non-phosphorylated (inactive) forms suitable for biochemical and structural studies thus facilitating the development of novel inhibitors.

## 1. Introduction

The search for lead compounds as part of drug discovery and optimization procedure is a complex and challenging process. The utilization of experimentally derived structures of target protein in complex with small molecules provides an accurate presentation, promoting the optimization of higher affinity and efficacy binders. The primary and one of the most relevant methods accelerating drug discovery is X-ray crystallography. In this regard, the advances in protein expression and purification, as well as rapid crystal data collection and analysis, vastly promote the field. The most critical restraint in such studies is the reproducibility in protein production and crystallization of well-diffracting crystals.

The cdc2-like kinases (CLKs) are dual-specificity kinases that undergo autophosphorylation on tyrosine residues [1] and phosphorylate their substrates exclusively on serine/threonine residues [2]. The CLK family consists of four conserved isoforms: CLK1, CLK2, CLK3, and CLK4, differing in their target specificities [1,3]. The CLK1 is composed of 484 amino acids and its catalytic domain (residues 148–484), based on its three-dimensional X-ray structure, exhibits a typical protein kinase fold [4]. The human CLK1 plays an important role in controlling alternative RNA splicing by regulating the cellular distribution and splicing activity of the SR family splicing factors via phosphorylation of their *C*-termini [2,5]. CLK1 was recently implicated in several

* Corresponding author. Department of Biological Chemistry, Alexander Silverman Institute of Life Sciences, The Edmond J. Safra Campus, The Hebrew University of Jerusalem, Jerusalem, 91904, Israel.
*E-mail address:* oded.livnah@huji.ac.il (O. Livnah).

https://doi.org/10.1016/j.pep.2020.105742
Received 20 May 2020; Received in revised form 3 August 2020; Accepted 26 August 2020
Available online 29 August 2020
1046-5928/

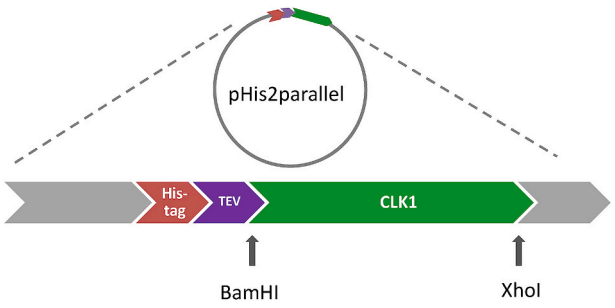


**Fig. 1.** Schematic representation of the T7 based vector used for CLK1 expression.

pathophysiological diseases such as Duchenne muscular dystrophy, Alzheimer's disease and cancers [6]. Moreover, in two independent genome-wide RNAi screens for host cell factors required for influenza A virus (IAV) replication, CLK1 was identified as one of the major factors involved in viral infection and replication, as in the case of alternative splicing of the influenza virus M2 gene during influenza infection and replication [7]. CLK1 was also found to influence adenoviral E1A gene alternative splicing in COS-1 cells [5], to increase gag protein expression in HIV-1 infected HeLa cells [8] and recently it was found to be essential for efficient replication of West Nile [9] and chikungunya viruses [10]. Wong et al. [8,11] have shown that different CLK1 inhibitors can decrease HIV replication in vitro by effecting mRNA processing. Similarly, it was found that specific CLK1 inhibitors influenced IAV mRNA splicing levels and hampered virus replication [12–14]. Furthermore, knockdown of CLK1 in primary cells and a mice model [14] was shown to reduce virus IAV replication. The involvement of CLK1 in these pathologies makes it a promising and essential target for developing specific inhibitors that can be utilized as novel anti-viral therapeutics.

The human kinome comprises of more than 500 protein kinases essential for cell function, playing a crucial role in primary signaling processes [15,16]. Their abnormal activities are associated with many diseases including life-threatening conditions [17]. These molecules are important targets for drug therapy and are regularly explored through

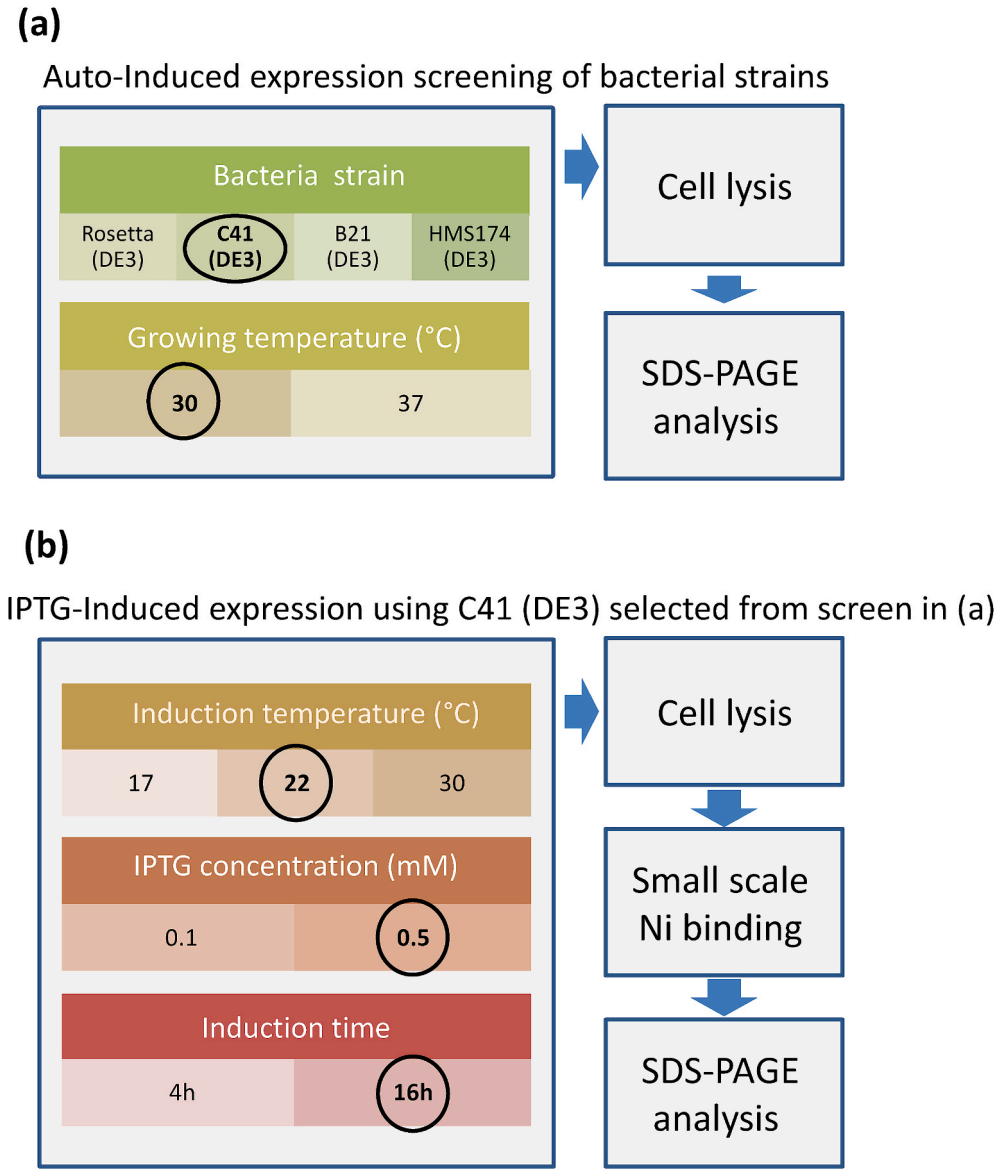


**Fig. 2.** Screening conditions for CLK1 expression. (a) Flow chart describing the process of screening for optimal conditions for soluble expression of CLK1 by auto-induction protocol. (b) Further refinement of CLK1 solubility and expression levels was obtained by calibrating IPTG-induced expression. Selected optimal conditions in (a) and (b) are surrounded by circles.

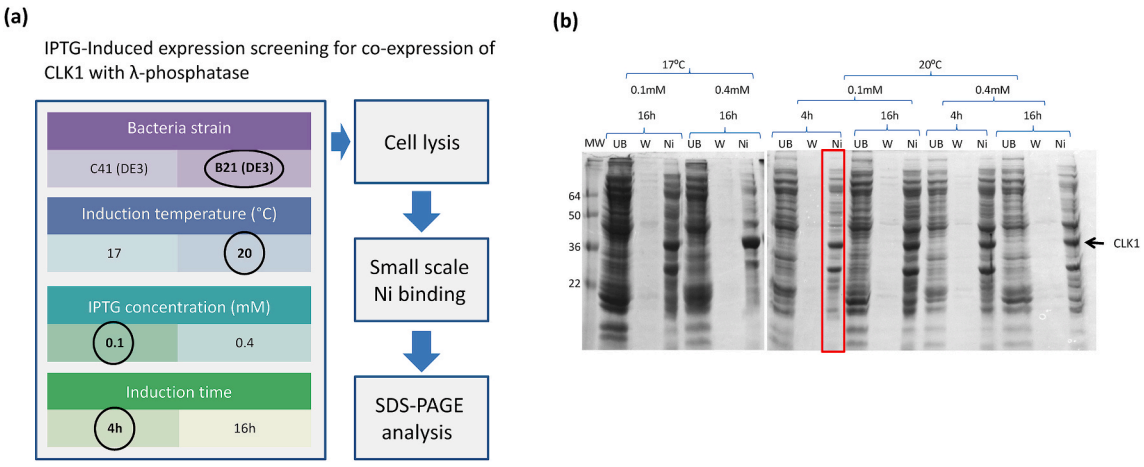


**Fig. 3.** Screening conditions for co-expression of CLK1 with λ-phosphatase in BL21 (DE3). (a) Flow chart describing the screening process using IPTG-induced expression protocol. (b) Cell lysates from cultures grown in different expression conditions were used for small scale affinity purification with Ni-NTA beads. Unbound (UB), wash (W) and eluted protein (Ni) were analyzed using SDS-PAGE. Molecular weight markers were loaded on the left lane. The selected optimal conditions are surrounded by circles in (a) and by a red rectangle in (b).

structural studies, mainly via X-ray crystallographic methods. For that purpose, one must obtain a highly purified homogeneous protein preparation. In this context, the preparation of kinases for structural studies using available expression systems could result in nonspecific or partial phosphorylation(s) leading to heterogeneous modifications on the surface of the protein. To overcome this predicament, careful progression in the expression and purification stages should be taken, by evaluating each step towards the desired outcome. In this study, we describe the preliminary stages of expression and purification of the kinase domain of human CLK1 aiming to obtain a reliable and reproducible source of crystallizable protein. This approach of kinase and phosphatase co-expression was previously used for the expression of other kinases, either by co-expressing on two separate plasmids [18,19] or by co-expressing on the same plasmid [20–23], and could be regarded as a common practice (benchmark) when producing protein kinases for reproducible crystallization assays and consequent structural studies.

## 2. Materials and methods

### 2.1. Cloning, expression, and purification of the kinase domain of human CLK1

The synthetic gene of CLK1 kinase domain (Accession Number: NP_004062, residues 148–484) was ordered from GeneScript, as codon optimized sequence for expression in *E. coli* cells. The CLK1 kinase domain was subcloned into the pET-based vector pHisParallel2 [24], using *Bam*HI and *Xho*I restriction enzymes, leaving 6xHis-tag and a TEV protease site at the 5' end of the cloned domain (Fig. 1).

In order to select the most suitable host for the soluble expression of the protein, sequence-verified pHis2CLK1 was transformed into several bacterial strains (BL21 (DE3), HMS174 (DE3), BL21 (DE3) Rosetta (EMD Novagen) and C41 (DE3) (Lucigen)), and subjected to standard auto-induction procedures [25]. In short, a single colony from each transformed bacterial strain was picked and grown for 16 h in 3 mL ZY medium (containing: 1% Bactotryptone (BD), 0.5% Bacto yeast extract (BD), 1 mM $MgSO_4$, 0.2% lactose, 0.05% glucose, 0.5% glycerol, 1xNPS (25 mM $(NH_4)_2SO_4$, 50 mM $KH_2PO_4$ and 50 mM $Na_2HPO_4$) and 100 μg/mL ampicillin), in an incubator shaker at temperatures of 30 °C and 37 °C. 1.5 mL culture of each condition was harvested, lysed in 750 μl of lysis buffer (50 mM Tris-HCl pH 7.5, 10% glycerol, 500 mM NaCl, 0.1% DDM, 1 mM PMSF, 0.2 mg/mL lysozyme, 10 mM $MgCl_2$, and 0.05 mg/mL DNase), and analyzed by SDS-PAGE. The selected strain was further calibrated for refining expression profile using IPTG induced expression protocol as follows: A single colony of freshly transformed bacteria was inoculated into 2 mL LB containing antibiotics. After 16 h the cells were diluted into 200 mL 2xYT media containing 1% glucose, 1xNPS and 100 μg/mL ampicillin. When the cell density reached the value of 0.7 at $OD_{600}$, the culture was divided into six flasks; each was incubated in one of the following temperatures: 17 °C, 22 °C and 30 °C, and induced by one of two IPTG (Merck, MBS420322) concentrations: 0.1 mM and 0.5 mM 1.5 mL samples of each condition were harvested after 4 and 16 h, lysed in 750 μl of lysis buffer, and 50 μl of Ni-NTA beads (Qiagen, 30,230) were added for small scale analysis of binding. Following 1 hour incubation at 4 °C, the beads were washed twice with 1 mL buffer (50 mM Tris-HCl pH 7.5, 10% glycerol, 500 mM NaCl). Elutions were preformed twice, with buffer containing 250 mM imidazole. Samples were loaded on 12% PAGE-SDS gels and analyzed by Coomassie stain and by Western blot with anti His-tag antibody (Novagen, 70796–3). Fig. 2a and b shows a schematic description of the screening procedure. For the large-scale production of CLK1 kinase domain, freshly transformed C41 (DE3) cells were plated on 100 μg/mL ampicillin selective LB agar plates. A single colony was used for a 16 h starter in 10 mL LB. The starter was then used to inoculate 1 L of 2xYT media containing 1% glucose, 1xNPS and 100 μg/mL ampicillin. When the cell density reached the value of 0.7 at $OD_{600}$, the culture was transferred into a 22 °C shaker and IPTG was added to a final concentration of 0.5 mM. The cells were harvested 16 h post induction.

### 2.2. Co-expression of CLK1 with λ-phosphatase

In the second attempt for expression, the pHis2CLK1 vector was co-transformed into BL21 (DE3) and into C41 (DE3) previously transformed with pACYC-LIC vector containing the λ-phosphatase gene (kindly provided by Prof. Stefan Knapp, SGC, Oxford [26]). To screen for the best expression conditions of CLK1 we co-expressed it with λ-phosphatase, to deplete unwanted phosphorylation. Protein production was induced in the following conditions: 0.1 mM or 0.4 mM of IPTG at 17 °C or 20 °C. 1.5 mL samples of each condition were harvested after 4 h and after 16 h, lysed, and the supernatant was used for small scale Ni binding, as previously described (Fig. 3a shows a schematic description of the screening procedure). Fractions from Ni purification were analyzed using SDS-PAGE (Fig. 3b).

For large-scale production of CLK1 co-expressed with λ-phosphatase, freshly transformed BL21 (DE3)- λ-phosphatase cells were plated on 34 μg/mL chloramphenicol and 100 μg/mL ampicillin selective LB agar plates. A single colony was used for a 16 h starter in 10 mL LB that was

then used to inoculate 1 L of 2xYT media containing 1% glucose, 1xNPS, 34 μg/mL chloramphenicol and 100 μg/mL ampicillin. When cell density reached 0.7 at $OD_{600}$, the culture was transferred into a 20 °C shaker and IPTG was added to a final concentration of 0.1 mM. Culture was harvested 4 h post induction.

In both expressions attempts (with and without λ-phosphatase) cells were harvested at 10,000 g for 10 min at 4 °C, and the dry pellet was immediately frozen at −80 °C until use. Cell pellet from 4 L culture was thawed on ice and immediately suspended in 400 mL buffer A (20 mM Hepes pH 7.5, 500 mM NaCl, 5% glycerol, 10 mM beta mercaptoethanol (βME), 10 mM imidazole), 50 μg/mL DNase, 0.2 mg/mL lysozyme, 0.5 mM PMSF, 1:500 protease inhibitor cocktail (Mercury, MBS539137), and 2 mM $MgCl_2$. Cell disruption was done using a microfluidizer (model M − 110 EHIS; Microfluidics Corp., Newton, MA), 21,000 psi, at 4 °C throughout the process. Insoluble cell debris was removed from the cell lysate by centrifugation at 4 °C for 20 min (15,000 g). Subsequently, the cleared lysate was filtered through 0.45 μm filter. All steps, from thawing the pellet to loading the lysate onto the column, were performed on ice.

### 2.3. Purification of CLK1 expressed without λ-phosphatase

Supernatant was loaded onto an equilibrated 5.1 × 1.0 cm column (4 mL) Ni-Sepharose FF column (GE-Healthcare) in an ÄKTA Explorer system (GE-Healthcare) at 4 °C. After loading, the column was washed with buffer A until low $OD_{280nm}$, and with buffer A with 30 mM imidazole. Finally, the His-tagged CLK1 was eluted by instantly increasing the imidazole concentration to 300 mM. Fractions were pooled according to $OD_{280/260}$ profile, and concentrated with a 10 kDa cut-off ultrafiltration device (PALL). CLK1 was further purified on a Superose 75 gel filtration column from GE Healthcare (100 × 1.6 cm, ~200 mL) pre-equilibrated with final storage buffer containing 20 mM HEPES 7.5, 500 mM NaCl, 10% glycerol and 10 mM βME. Fractions containing CLK1 monomer (according to $OD_{280/260}$ profile) were pooled, aliquoted and kept frozen at −80 °C until crystallization assays.

### 2.4. Purification of CLK1 co-expressed with λ-phosphatase

Supernatant was loaded onto an equilibrated 8 × 1.6 cm column (16 mL) Ni-Sepharose FF column (GE-Healthcare) in an ÄKTA Explorer system (GE-Healthcare) at 4 °C. After loading, the column was washed with buffer A until low $OD_{280nm}$, and with buffer A containing 30 mM imidazole. Finally, the His-tagged CLK1 was eluted by increasing the imidazole concentration to 500 mM. Fractions were pooled according to $OD_{280/260}$ profile, supplemented with 50 mM arginine, 50 mM glutamate and 10 mM DTT to avoid aggregation [27–29], and concentrated with a 10 kDa cut-off ultrafiltration device (PALL). The protein was then incubated with TEV protease (1:20 v:v) for overnight dialysis at 4 °C against buffer A.

The TEV protease was expressed using pRK793 plasmid kindly provided by Dr. David Waugh and purified as previously described [30]. CLK1 was further purified on a Sephacryl S100 gel filtration column from GE Healthcare (100 × 2.6 cm) pre-equilibrated with GF buffer containing 20 mM Tris-HCl 8.5, 100 mM NaCl, 2 mM EDTA, 5% glycerol and 5 mM βME. Fractions containing the soluble monomeric CLK1 were pooled and subsequently loaded onto a 10 × 1 cm Res 15Q anion-exchange column (GE Healthcare) equilibrated with AEX buffer, containing 20 mM Tris-HCl 8.5, 50 mM NaCl, 2 mM EDTA, 5% glycerol and 5 mM βME. Last ion-exchange column separated two different CLK1 populations: the first one, which did not bind to the column (unbound fraction) and the second one, which was eluted in higher NaCl concentration (see result section for crystallization information). Each of the two eluted CLK1 populations was dialyzed overnight against a buffer suitable for crystallization, containing 50 mM Hepes pH 7.5, 0.5 M NaCl, 5% glycerol, 50 mM arginine, 50 mM glutamate and 10 mM DTT. Purified CLK1 solution was then concentrated to 8 mg/mL and kept frozen at −80 °C until subjected to crystallization assays. CLK1 concentration was determined using Abs 0.1% (=1 g/L) of 1.060 at 280 nm.

### 2.5. SDS-PAGE and Western blot analysis

Samples from different purification steps were boiled in the presence of reducing buffer (50% glycerol, 10% SDS, 3.8% DTT, 100 mM Tris-HCl pH 6.8 and bromophenol blue) and resolved on Mini-Protean TGX Stain-Free 4–20% gels (Bio-Rad, 4568096). Precision Plus Protein All Blue Standards (Bio-Rad, 1610737) were used as molecular weight markers. Gels were stained with Instant Blue (Expedeon) and visualized using ChemiDoc XRS camera (Bio-Rad). For Western blot analysis, total protein was visualized using ChemiDoc XRS camera, Image Lab software, Stain Free Gel protocol. The proteins were then transferred to a nitrocellulose membrane (using BioRad trans-blot turbo) and blocked with blocking solution containing 10% glycerol, 3% BSA, 1% skim milk, 1 M L-glucose and 0.5% Tween-20 in Tris buffer saline at 22 °C for 1 h. Membranes were incubated with mouse *anti*-phosphotyrosine (clone 4G10, Merck Millipore) and mouse *anti*-phosphothreonine (clone 42h4, Cell Signaling) at a 1:1000 dilution in antibody incubation buffer (5% skim milk, 0.05% Tween-20 in Tris buffer saline) at 22 °C for 1 h. Membranes were washed three times for 10 min each with TBS-T (10 mM Tris, 150 mM NaCl and 0.1% Tween-20). Goat anti-mouse IgG (Jackson Immunoresearch, 115-035-003) was added at a 1:5000 dilution in antibody incubation buffer and incubated at 22 °C for 1 h. Membranes were washed three times for 10 min with TBS-T. Bands were visualized following addition of EZ-ECL (Biological Industries, 20-500-120) using ChemiDoc XRS + camera (Bio-Rad).

### 2.6. Crystallization data collection and processing of CLK1

We have examined the grade of CLK1 preparation suitable for crystallization by repeating the already available conditions for CLK1 in complex with the KH-CB19 inhibitor [4]. In this regard, crystals in the complexed form were obtained by the sitting drop vapor diffusion method. The KH-CB19 inhibitor was solubilized in DMSO (100 mM) and added to the protein solution containing 8 mg/mL CLK1 in its final solution (see purification segment) at the 1:100 ratio. Crystals of the CLK1: KH-CB19 complex were obtained at 4 °C at a 2:1 protein-reservoir with reservoir solution consisting of 2.1–2.3 M sodium malate at the pH range of 6.0–7.0 as previously reported [4]. Crystals appeared within 2 days and grew to the final size within a week. Prior to freezing, crystals were suspended in a cryo solution containing 20% ethylene glycol and the reservoir solution, mounted on a MiteGen loop and flash cooled in liquid nitrogen. Crystallographic data were collected at the European Synchrotron Radiation Facility (ESRF), Grenoble, France on beamline ID29 [31] at the temperature of 100 K, using an Oxford Cryosystem Cryostream cooling device. The data were indexed, integrated and scaled using the HKL2000 suite [32].

Screens for additional crystallization conditions were carried at the HTX lab in Grenoble. The initial hits were refined and CLK1 was crystallized in the sitting drop vapor diffusion method, the reservoir containing 24% polyethylene glycol 3350, 200 mM $MgCl_2{\cdot}6H_2O$, 100 mM BisTris pH 6–6.5. The crystallization drop contained 1:1 ratio of protein-reservoir, incubated at 20 °C. The cryo solution for these crystals contained 20% glycerol and the reservoir solution.

## 3. Results and discussion

### 3.1. Protein expression and purification

The human CLK1 gene is 1455 bp in length and encodes a 484 amino acids protein. A synthetic gene corresponding to the kinase domain of CLK1, was sub-cloned into the expression vector pHis2parallel [24]. Using the auto-induction protocol we have screened expression in several bacterial strains (Fig. 2a) and final expression conditions were

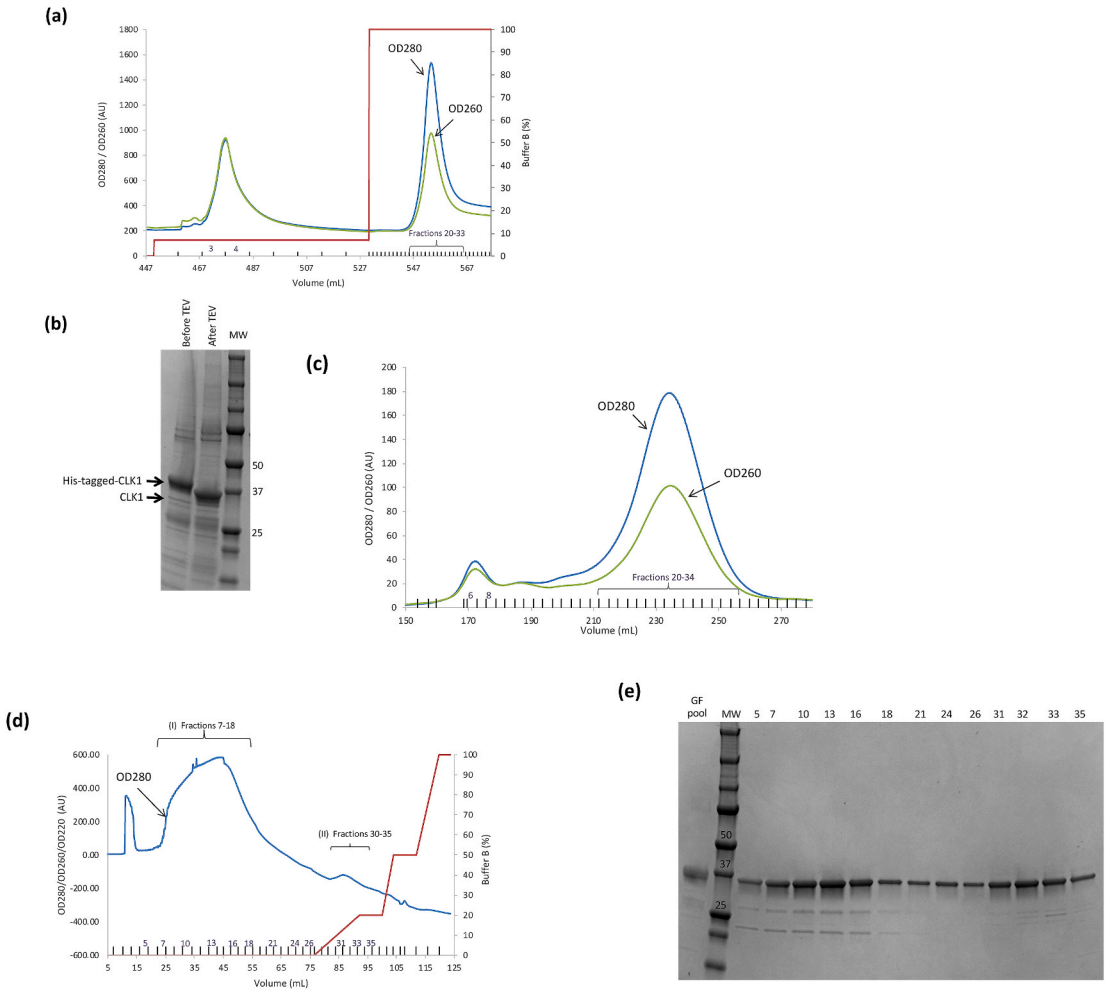


**Fig. 4.** The purification process of CLK1. (a) Ni-Column chromatogram. Elevating the imidazole concentration to 500 mM resulted in the elution of CLK1 (second peak, fractions 20–33). (b) SDS-PAGE analysis of fractions collected before TEV cleavage (1st lane) and after TEV cleavage (2nd lane). (c) Gel filtration chromatogram where CLK1 is eluted in the second peak (fraction 20–34). (d) Anion-exchange chromatogram. Two CLK1 populations were separated by this column. Only the unbound pool I (fraction 7–18) resulted in crystals, whereas pool II (fractions 30–35), eluted by elevating NaCl concentration, did not result in crystal formation. (e) SDS-PAGE analysis of fractions collected before (1st lane) and during anion-exchange column purification. The fraction number above each lane corresponds to the fraction number in (d).

selected by screening various IPTG concentrations, temperatures and harvest time. We found that the highest yield of soluble CLK1 was obtained when using C41 (DE3) induced with 0.5 mM IPTG, harvested 16 h post induction at 22 °C (Fig. 2b). The C41and C43 strains [33] are known for supporting the expression of otherwise toxic proteins. Indeed, in our case, we were able to obtain higher levels of expressed protein in this strain, probably due to overcoming the toxic effects of the kinase that were more evident in the other strains in the screen (data not shown). However, despite the high expression level and purity of the protein, the CLK1 produced in this procedure did not yield crystals, most probably due to non-homogeneous phosphorylation of the protein. In this regard, Western blot analysis using *anti*-phosphothreonine and *anti*-phosphotyrosine antibodies clearly showed that the CLK1 is phosphorylated on tyrosine and threonine residues (Fig. 5a and b, right panel, lane 4). This is an expected outcome since CLK1 has autophosphorylation capabilities on Tyr, and cross phosphorylation on Ser and Thr residues [34].

We attempted to produce a more homogeneous non-phosphorylated CLK1, by co-expression of CLK1 with λ-phosphatase. To obtain this we have transformed expressing bacteria with both pACYC-LIC λ-phosphatase [26] and pHis2CLK1. Several expression conditions were screened as detailed in the materials and methods section (Fig. 3a). Best results (soluble and purified protein) were obtained when constructs were transformed into BL21 (DE3) cells, induced with 0.1 mM IPTG at $OD_{600} = 0.7$, grown at 20 °C and harvested 4 h post induction (Fig. 3b). Induction with 0.4 mM IPTG and growing for 16 h at 17 °C also resulted in high levels of soluble CLK1 (Fig. 3b). However, once obtaining well-diffracting crystals from CLK1 grown in 20 °C, we continued with these conditions.

We then used the calibrated conditions to scale-up CLK1 production in 4 L culture. In the first step of purification CLK1 was loaded on Ni-sepharose FF column and eluted with 500 mM imidazole (Fig. 4a). In order to avoid protein aggregation, samples containing CLK1 were supplemented with DTT, arginine and glutamate [27–29]. The pool was then subjected to an overnight digestion with TEV protease, to remove the *N*-terminus His-tag from the CLK1. The TEV cleavage was verified by SDS-PAGE analysis (Fig. 4b). In our first purification attempts, TEV cleavage was followed by a negative-Nickel column in order to remove the un-cleaved His-tagged CLK1. However, SDS-PAGE analysis showed that this step is redundant, since the TEV digestion of CLK1 His-tag was complete (Fig. 4b).

The *N*-terminus cleaved CLK1 was then loaded on gel filtration column. CLK1 was eluted in two peaks (Fig. 4c), where the first peak contained the aggregated protein and the second peak corresponds to the CLK1 monomer. The fractions containing the monomer were then pooled and loaded on an anion-exchange column. Two separate peaks

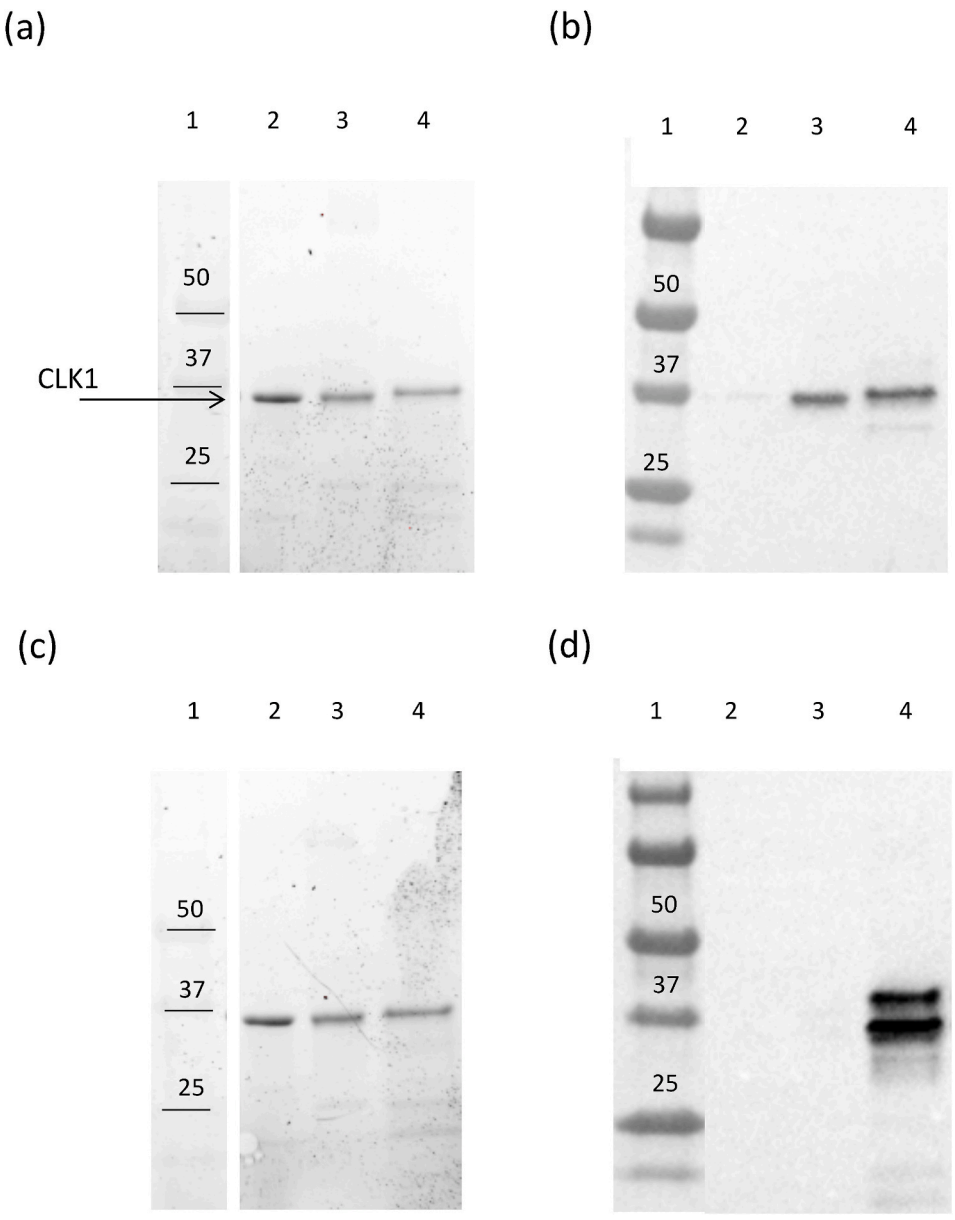


**Fig. 5.** Phosphorylation profile of CLK1. CLK1 was dephosphorylated by co-expression in BL21 (DE3) with λ-phosphatase. (a, c) Purified CLK1 fractions were loaded on 4–20% TGX Stain-Free precast gels (Bio-Rad). Lane 1: molecular weight markers; Lanes 2–3: ion-exchange column fractions (pools I and II, see Fig. 4d); lane 4: phosphorylated form of CLK1, expressed without λ-phosphatase. Total protein was visualized using Bio-Rad Stain Free Gels with the Stain free gel protocol (Image Lab software) (a and c) and then probed against *anti*-phosphothreonine (b) and against *anti*-phosphotyrosine (d), to detect phosphorylation levels. The two bands detected on lane 4 in (d), are due to incomplete TEV cleavage.

could be distinguished on the anion exchange chromatogram (Fig. 4d) and by SDS-PAGE (Fig. 4e). The first peak corresponds to a CLK1 population that did not bind to the column. A second population was eluted by a NaCl gradient between 50 mM and 200 mM. These two populations were pooled separately and subjected to crystallization assays, but only the first population (the unbound fractions) resulted in crystals.

Examination of the phosphorylation profile by Western blot analysis, using *anti*-phosphotyrosine and *anti*-phosphothreonine antibodies, showed that the unbound fraction that resulted in crystals, contained undetectable levels of threonine and tyrosine phosphorylation (Fig. 5b and d, lane 2). On the other hand, in the second population that did not form crystals, the threonine was phospohorylated in similar intensity as the CLK1 expressed without *λ*-phosphatase (Fig. 5b, lane 3 and 4 respectively). This indicates that the co-expression of CLK1 with *λ*-phosphatase dramatically decreased the phosphorylation of the tyrosine and partially decreased the phosphorylation of threonine. Thus, the failure to crystalize the second populations may be attributed to heterogeneity in CLK1 phosphorylation pattern. In summary, a typical purification run of CLK1 from a 4 L culture, including Ni-sepharose, gel filtration and a final anion-exchange column from which only the unbound population was collected resulting in approximately 8 mg of homogeneous and crystallizable protein.

Since CLK1 has a tendency to aggregate during purification, all procedures were performed using protocols developed in our group for purification of prone to aggregate proteins [28,29]. In general, physicochemical environment such as buffers, pH value, and the use of chosmotropes or chaotropes additives should be screened in the purification development of such proteins. It should be noted that the cell-disruption conditions (including the apparatus type) might introduce batch to batch variability, leading to irreproducibility. Hence, for this type of 'delicate' proteins, aggregation problems can often occur at different stages of the purification process. In this regard, an intriguing observation where a change of the cell disruption apparatus, from a gentler disruption to a somewhat aggressive (higher pressure and probable increase in temperature) resulted in a non-stable CLK1 with an increased tendency to aggregate and thus unsuitable for crystallization assays. Moreover, the procedures require rapid manipulation at 4 °C, as well as avoiding protein overcrowding during purification steps. Emphasis should be given to designing a "rapid strategy of purification", where proteins must be produced and stored as fast as possible. To

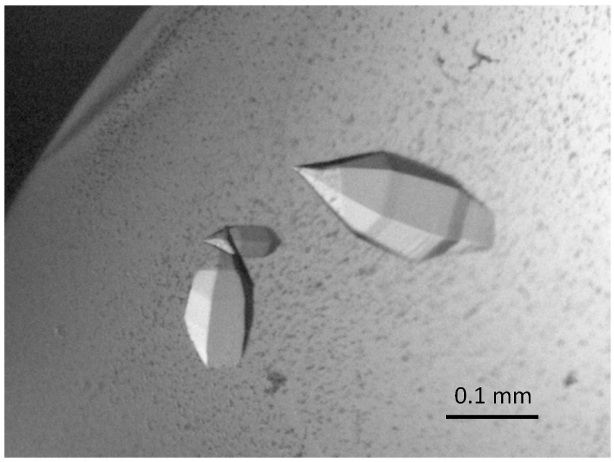


**Fig. 6.** Crystals of CLK1 complexed with the KH-CB19 inhibitor. The black bar indicates the size of 0.1 mm.

**Table 1**
Data collection and processing statistics.

| ESRF Beamline | ID29 |
|---|---|
| Wavelength (Å) | 0.930 |
| Temperature | 100 K |
| Crystal-detector distance (mm) | 258.56 |
| Rotation range per image | 0.2° |
| Exposure time per image (sec) | 0.1 |
| Total no. of images | 880 |
| Space group | $P6_522$ |
| Cell parameters | $a = 68.8$ Å $c = 285.0$ Å |
| Resolution range (Å) (Outer shell) | 50.0–1.65 (1.68–1.65) |
| Unique reflections | 49,449 (2432) |
| Completeness | 99.6 (99.9) |
| Rsym | 0.103 (0.922) |
| Redundancy | 6.5 (6.5) |
| I/σ | 16 (1.64) |
| CC(1/2) | 0.98 (0.59) |

achieve this goal, optimization of each of the purification steps should be performed prior to scale-up.

### 3.2. Crystallization of CLK1

The crystals of the CLK1 complexed with the KH-CB19 inhibitor (Fig. 6) were characterized and belong to the hexagonal $P6_522$ space group, with unit cell parameters a = 68.8 Å, c = 285.0 Å containing one CLK1 molecule in the asymmetric unit with the Vm value of 2.52 $Å^3$/Da (Table 1). The current space group and cell parameters differ from the previously published complex (PDB entry 2VAG) which was the monoclinic C2 (a = 90.9 Å, b = 64.1 Å c = 78.9 Å, b = 118.2°) [4] although highly similar crystallization conditions were employed. The structure was solved via molecular replacement methods using PHASER [35] implemented in CCP4i [36] and is being analyzed. In this regard, there is a clear electron density indicting the presence of the inhibitor in the active site (not shown).

## 4. Conclusions

In this work, we devised a method for the expression and purification of CLK1 suitable for crystallization assays. Our general aim was to obtain a homogeneous preparation of CLK1 in order to achieve reproducible results in crystallization and co-crystallization with potential inhibitors. In order to cleave all possible phosphates from the phosphorylation sites, we have co-expressed CLK1 with λ-phosphatase in the same *E. coli* host strain. By doing so, the inherent heterogeneity was substantially decreased as shown via Western blot analysis. We extensively screened for numerous expression conditions and purification protocols that finally resulted in crystals used for structure analysis of CLK1 complexed with small molecule compounds. In this context, the third and final anion exchange polishing purification step resulted in a homogeneous, reproducible and crystallizable CLK1. It is thus highly recommended to analyze and validate the protein homogeneity and monomodality using different criteria such as size, charge and light scattering methods. The methodology that was used in this work and by others [33] could be adopted as a standard approach for producing kinases in their non-phosphorylated inactive forms for biological and biochemical purposes as well as for obtaining viable targets for successful and reproducible crystallization attempts.

## Authors statement

The authors have no competing interests to declare.

## Declaration of competing interest

None.

## Acknowledgments

We thank the ESRF staff for their help in maintaining this excellent facility, the HTX lab in Grenoble with the support of BioStructX_4232. This paper is based on work fully supported by the ANTIFLU research project (Innovative anti-influenza drugs excluding viral escape) funded under the European Community's Seventh Framework Programme (FP7/2007–2013) under grant agreement No. 259842.

## Appendix A. Supplementary data

Supplementary data to this article can be found online at https://doi.org/10.1016/j.pep.2020.105742.

## References

[1] O. Nayler, S. Stamm, A. Ullrich, Characterization and comparison of four serine- and arginine-rich (SR) protein kinases, Biochem. J. 326 (Pt 3) (1997) 693–700.
[2] K. Colwill, T. Pawson, B. Andrews, J. Prasad, J.L. Manley, J.C. Bell, P.I. Duncan, The Clk/Sty protein kinase phosphorylates SR splicing factors and regulates their intranuclear distribution, EMBO J. 15 (1996) 265–275.
[3] J. Hanes, H. von der Kammer, J. Klaudiny, K.H. Scheit, Characterization by cDNA cloning of two new human protein kinases. Evidence by sequence comparison of a new family of mammalian protein kinases, J. Mol. Biol. 244 (1994) 665–672.
[4] O. Fedorov, K. Huber, A. Eisenreich, P. Filippakopoulos, O. King, A.N. Bullock, D. Szklarczyk, L.J. Jensen, D. Fabbro, J. Trappe, U. Rauch, F. Bracher, S. Knapp, Specific CLK inhibitors from a novel chemotype for regulation of alternative splicing, Chem. Biol. 18 (2011) 67–76.
[5] P.I. Duncan, D.F. Stojdl, R.M. Marius, J.C. Bell, In vivo regulation of alternative pre-mRNA splicing by the Clk1 protein kinase, Mol. Cell Biol. 17 (1997) 5996–6001.
[6] M. Murar, J. Dobias, P. Sramel, G. Addova, G. Hanquet, A. Bohac, Novel CLK1 inhibitors based on N-aryloxazol-2-amine skeleton - a possible way to dual VEGFR2 TK/CLK ligands, Eur. J. Med. Chem. 126 (2017) 754–761.
[7] R. Konig, S. Stertz, Y. Zhou, A. Inoue, H.H. Hoffmann, S. Bhattacharyya, J. G. Alamares, D.M. Tscherne, M.B. Ortigoza, Y. Liang, Q. Gao, S.E. Andrews, S. Bandyopadhyay, P. De Jesus, B.P. Tu, L. Pache, C. Shih, A. Orth, G. Bonamy, L. Miraglia, T. Ideker, A. Garcia-Sastre, J.A. Young, P. Palese, M.L. Shaw, S. K. Chanda, Human host factors required for influenza virus replication, Nature 463 (2010) 813–817.
[8] R. Wong, A. Balachandran, A.Y. Mao, W. Dobson, S. Gray-Owen, A. Cochrane, Differential effect of CLK SR Kinases on HIV-1 gene expression: potential novel targets for therapy, Retrovirology 8 (2011) 47.
[9] M.N. Krishnan, A. Ng, B. Sukumaran, F.D. Gilfoy, P.D. Uchil, H. Sultana, A.L. Brass, R. Adametz, M. Tsui, F. Qian, R.R. Montgomery, S. Lev, P.W. Mason, R.A. Koski, S. J. Elledge, R.J. Xavier, H. Agaisse, E. Fikrig, RNA interference screen for human genes associated with West Nile virus infection, Nature 455 (2008) 242–245.
[10] A. Karlas, S. Berre, T. Couderc, M. Varjak, P. Braun, M. Meyer, N. Gangneux, L. Karo-Astover, F. Weege, M. Raftery, G. Schonrich, U. Klemm, A. Wurzlbauer, F. Bracher, A. Merits, T.F. Meyer, M. Lecuit, A human genome-wide loss-of-

function screen identifies effective chikungunya antiviral drugs, Nat. Commun. 7 (2016) 11320.
[11] R.W. Wong, A. Balachandran, M. Haaland, P. Stoilov, A. Cochrane, Characterization of novel inhibitors of HIV-1 replication that function via alteration of viral RNA processing and rev function, Nucleic Acids Res. 41 (2013) 9471–9483.
[12] M. Zu, C. Li, J.S. Fang, W.W. Lian, A.L. Liu, L.S. Zheng, G.H. Du, Drug discovery of host CLK1 inhibitors for influenza treatment, Molecules 20 (2015) 19735–19747.
[13] A. Karlas, N. Machuy, Y. Shin, K.P. Pleissner, A. Artarini, D. Heuer, D. Becker, H. Khalil, L.A. Ogilvie, S. Hess, A.P. Maurer, E. Muller, T. Wolff, T. Rudel, T. F. Meyer, Genome-wide RNAi screen identifies human host factors crucial for influenza virus replication, Nature 463 (2010) 818–822.
[14] A. Artarini, M. Meyer, Y.J. Shin, K. Huber, N. Hilz, F. Bracher, D. Eros, L. Orfi, G. Keri, S. Goedert, M. Neuenschwander, J. von Kries, Y. Domovich-Eisenberg, N. Dekel, I. Szabadkai, M. Lebendiker, Z. Horvath, T. Danieli, O. Livnah, O. Moncorge, R. Frise, W. Barclay, T.F. Meyer, A. Karlas, Regulation of influenza A virus mRNA splicing by CLK1, Antivir. Res. 168 (2019) 187–196.
[15] G. Manning, D.B. Whyte, R. Martinez, T. Hunter, S. Sudarsanam, The protein kinase complement of the human genome, Science 298 (2002) 1912–1934.
[16] P. Jenardhanan, M. Panneerselvam, P.P. Mathur, Targeting kinase interaction networks: a new paradigm in PPI based design of kinase inhibitors, Curr. Top. Med. Chem. 19 (2019) 467–485.
[17] P. Bamborough, System-based drug discovery within the human kinome, Expet Opin. Drug Discov. 7 (2012) 1053–1070.
[18] R. Kristelly, T.W. Qiu, N.J. Gunn, D.B. Scanlon, T.D. Mulhern, Bacterial expression and purification of active hematopoietic cell kinase, Protein Expr. Purif. 78 (2011) 14–21.
[19] M.A. Seeliger, M. Young, M.N. Henderson, P. Pellicena, D.S. King, A.M. Falick, J. Kuriyan, High yield bacterial expression of active c-Abl and c-Src tyrosine kinases, Protein Sci. 14 (2005) 3135–3139.
[20] A.M. Garrote, P. Redondo, G. Montoya, I.G. Munoz, Purification, crystallization and preliminary X-ray diffraction analysis of the kinase domain of human tousled-like kinase 2, Acta Crystallogr F Struct Biol Commun 70 (2014) 354–357.
[21] S. Bhoir, A. Shaik, V. Thiruvenkatam, S. Kirubakaran, High yield bacterial expression, purification and characterisation of bioactive Human Tousled-like Kinase 1B involved in cancer, Sci. Rep. 8 (2018) 4796.
[22] W. Wang, A. Marimuthu, J. Tsai, A. Kumar, H.I. Krupka, C. Zhang, B. Powell, Y. Suzuki, H. Nguyen, M. Tabrizizad, C. Luu, B.L. West, Structural characterization of autoinhibited c-Met kinase produced by coexpression in bacteria with phosphatase, Proc. Natl. Acad. Sci. U. S. A. 103 (2006) 3563–3568.
[23] S.K. Albanese, D.L. Parton, M. Isik, L. Rodriguez-Laureano, S.M. Hanson, J.M. Behr, S. Gradia, C. Jeans, N.M. Levinson, M.A. Seeliger, J.D. Chodera, An open library of human kinase domain constructs for automated bacterial expression, Biochemistry 57 (2018) 4675–4689.
[24] P. Sheffield, S. Garrard, Z. Derewenda, Overcoming expression and purification problems of RhoGDI using a family of "parallel" expression vectors, Protein Expr. Purif. 15 (1999) 34–39.
[25] F.W. Studier, Protein production by auto-induction in high density shaking cultures, Protein Expr. Purif. 41 (2005) 207–234.
[26] A.N. Bullock, S. Das, J.E. Debreczeni, P. Rellos, O. Fedorov, F.H. Niesen, K. Guo, E. Papagrigoriou, A.L. Amos, S. Cho, B.E. Turk, G. Ghosh, S. Knapp, Kinase domain insertions define distinct roles of CLK kinases in SR protein phosphorylation, Structure 17 (2009) 352–362.
[27] A.P. Golovanov, G.M. Hautbergue, S.A. Wilson, L.Y. Lian, A simple method for improving protein solubility and long-term stability, J. Am. Chem. Soc. 126 (2004) 8933–8939.
[28] M. Lebendiker, T. Danieli, Production of prone-to-aggregate proteins, FEBS Lett. 588 (2014) 236–246.
[29] M. Lebendiker, M. Maes, A. Friedler, A screening methodology for purifying proteins with aggregation problems, Methods Mol. Biol. 1258 (2015) 261–281.
[30] J.E. Tropea, S. Cherry, D.S. Waugh, Expression and purification of soluble His(6)-tagged TEV protease, Methods Mol. Biol. 498 (2009) 297–307.
[31] D. de Sanctis, A. Beteva, H. Caserotto, F. Dobias, J. Gabadinho, T. Giraud, A. Gobbo, M. Guijarro, M. Lentini, B. Lavault, T. Mairs, S. McSweeney, S. Petitdemange, V. Rey-Bakaikoa, J. Surr, P. Theveneau, G.A. Leonard, C. Mueller-Dieckmann, ID29: a high-intensity highly automated ESRF beamline for macromolecular crystallography experiments exploiting anomalous scattering, J. Synchrotron Radiat. 19 (2012) 455–461.
[32] Z. Otwinowski, W. Minor, Processing of X-Ray Diffraction Data Collected in Oscillation Mode, Methods in Enzymology, Academic Press, New York, 1997, pp. 307–326.
[33] T.D. Melo-Hanchuk, P.F. Slepicka, G.V. Meirelles, F.L. Basei, D.V. Lovato, D. C. Granato, B.A. Pauletti, R.R. Domingues, A.F.P. Leme, A.L. Pelegrini, G. Lenz, S. Knapp, J.M. Elkins, J. Kobarg, NEK1 kinase domain structure and its dynamic protein interactome after exposure to Cisplatin, Sci. Rep. 7 (2017) 5445.
[34] Y. Ben-David, K. Letwin, L. Tannock, A. Bernstein, T. Pawson, A mammalian protein kinase with potential for serine/threonine and tyrosine phosphorylation is related to cell cycle regulators, EMBO J. 10 (1991) 317–325.
[35] A.J. McCoy, R.W. Grosse-Kunstleve, P.D. Adams, M.D. Winn, L.C. Storoni, R. J. Read, Phaser crystallographic software, J. Appl. Crystallogr. 40 (2007) 658–674.
[36] E. Potterton, P. Briggs, M. Turkenburg, E. Dodson, A graphical user interface to the CCP4 program suite, Acta Crystallogr D Biol Crystallogr 59 (2003) 1131–1137.